

# Biodegradable poly(lactide-co-glycolide) coatings on magnesium alloys for orthopedic applications

Nicole J. Ostrowski · Boeun Lee · Abhijit Roy ·  
Madhumati Ramanathan · Prashant N. Kumta

Received: 24 June 2012 / Accepted: 18 September 2012 / Published online: 10 October 2012  
© Springer Science+Business Media New York 2012

**Abstract** Polymeric film coatings were applied by dip coating on two magnesium alloy systems, AZ31 and Mg4Y, in an attempt to slow the degradation of these alloys under in vitro conditions. Poly(lactic-co-glycolic acid) polymer in solution was explored at various concentrations, yielding coatings of varying thicknesses on the alloy substrates. Electrochemical corrosion studies indicate that the coatings initially provide some corrosion protection. Degradation studies showed reduced degradation over 3 days, but beyond this time point however, do not maintain a reduction in corrosion rate. Scanning electron microscopy indicates inhomogeneous coating durability,

with gas pocket formation in the polymer coating, resulting in eventual detachment from the alloy surface. In vitro studies of cell viability utilizing mouse osteoblast cells showed improved biocompatibility of polymer coated substrates over the bare AZ31 and Mg4Y substrates. Results demonstrate that while challenges remain for long term degradation control, the developed polymeric coatings nevertheless provide short term corrosion protection and improved biocompatibility of magnesium alloys for possible use in orthopedic applications.

## 1 Introduction

Historically, within the orthopedic market, fixation and repair have been limited to implantation of inert alloys, such as titanium and stainless steel, to immobilize and heal damaged bone [1–3]. Magnesium and magnesium-based alloys pose a bright prospect for use in orthopedic and craniofacial repair applications since these alloys not only display physical properties strikingly similar to natural bone but also exhibit the unique ability to degrade in vivo [1, 4–6]. As a result, these alloys are potentially promising candidates for orthopedic fixation plates and screw device. Such implants that degrade on demand in vivo following completion of their primary function to providing support to the underlying fractured bone or healing of the non-union are indeed desirable because this type of implant reduces the chance of long term complications associated with permanent implants, including foreign body response, delayed type hypersensitivity, and painful secondary removal surgery [1, 7]. Consequently, research into the potential of magnesium-based alloys for implants that degrade in this manner has increased exponentially in the past 5 years. The current barrier to clinical implementation

---

N. J. Ostrowski · B. Lee · A. Roy · M. Ramanathan ·  
P. N. Kumta (✉)  
Department of Bioengineering, University of Pittsburgh,  
Pittsburgh, PA 15261, USA  
e-mail: pkumta@pitt.edu

N. J. Ostrowski · B. Lee · A. Roy · M. Ramanathan ·  
P. N. Kumta  
Swanson School of Engineering and School of Dental Medicine,  
University of Pittsburgh, 849 Benedum Hall, Pittsburgh,  
PA 15261, USA

P. N. Kumta  
Department of Chemical and Petroleum Engineering,  
University of Pittsburgh, Pittsburgh, PA 15261, USA

P. N. Kumta  
Department of Mechanical Engineering and Materials Science,  
University of Pittsburgh, Pittsburgh, PA 15261, USA

P. N. Kumta  
Center for Craniofacial Regeneration, University of Pittsburgh,  
Pittsburgh, PA 15261, USA

P. N. Kumta  
Center for Complex Engineered Multifunctional Materials  
(CCEMM), University of Pittsburgh, Pittsburgh, PA 15261, USA

for magnesium alloys is the aggressive degradation rate, accompanied by hydrogen gas evolution, and limited bioactivity [7, 8]. This hydrogen gas evolution results in undesirable gas pocket formation near the site of implantation. The corrosion of magnesium *in vivo* results in hydrogen gas evolution following the general reaction:



It can be seen from Eq. 1 that the dissolution of one atom of magnesium generates one molecule of hydrogen gas [9]. It is also generally accepted that magnesium and the hydroxide ions will react to form  $\text{Mg}(\text{OH})_2$  passivation layer on the surface of the implant. However, this layer is not highly stable and that magnesium alloys are susceptible to pitting corrosion [2].

Strategies to limit degradation rate *in vivo* include exploring unique alloying elements, processing strategies and applying surface coatings. Alloying and improvements in processing methodologies may obtain slower degradation rates, but are not likely to drastically improve the surface bioactivity of the implant, which can ultimately affect osseointegration and new bone growth [8, 10]. The utilization of surface coating is thus of great interest, as coatings have the potential to both slow degradation and increase the biocompatibility of implants. Specifically of interest are calcium-phosphate based coatings due to their structural similarity to the mineralized component of natural bone, and degradable polymeric coatings [6, 11–15]. Coatings of degradable polymers can not only act as a corrosion barrier, but can be used to deliver drugs, genes and growth factors at the body-implant interface [16]. Among the many natural and synthetic polymers explored poly(lactide-co-glycolide) (PLGA) has numerous justifications for use as a coating owing to their high biocompatibility, clearance through FDA for numerous devices, well explored drug delivery capabilities and ability to tailor *in vivo* degradation rates with metabolically digestible degradation products [17–20]. The integration of PLGA on the surface of magnesium alloys could therefore potentially serve to inhibit corrosion and additionally act as a scaffold to elude antibiotic agents, such as cefoxitin sodium, or growth factors, such as BMP-2 [21, 22]. Previously, Li et al. [23] explored a high molecular weight 90:10 PLGA on a magnesium—6 wt% zinc alloy, and showed some corrosion protection of the alloy, as demonstrated by polarization curves and electrochemical impedance spectroscopy (EIS). Surprisingly, the authors determined that a thinner coating would provide more protection against corrosion than a thicker coating. The authors speculated that the thinner coating is sufficient to passivate the alloy surface and that a thicker coating contains more defects than the thinner coating while providing no additional passivation, thus leading to an inferior corrosion protection

profile for the thicker coating. Xu et al. [24] and Lu et al. [25] have recently reported the incorporation of PLGA, films or spheres, into composite coatings for drug-release purposes.

In this study, a mid-range molecular weight 50:50 PLGA is coated on to two magnesium alloy systems, AZ31 (96 % Mg, 3 % Al and 1 % Zn by weight) and Mg4Y (96 % Mg and 4 % Y, by weight). It should be noted that this is the first report of PLGA coatings on AZ31 or Mg-Y alloy systems to the best of our knowledge. The present study was conducted in order to evaluate the potential of PLGA coatings to slow the corrosion and increase the biocompatibility of the AZ31 and Mg4Y alloys. The successful implementation of PLGA for this purpose could lead to the use of PLGA as a one-step, multifunctional coatings for magnesium-based alloys for use in orthopedic applications requiring biocompatibility and time dependent corrosion protection.

## 2 Materials and methods

### 2.1 Materials and sample preparation

Hot rolled AZ31 alloy was acquired from Alfa Aesar (Ward Hill, MA, USA) and was used as received. Mg4Y was acquired from GKSS Research Institute (Geesthacht, Germany) in ingot form, graciously provided by Dr. Norbert Hort, and further homogenized by heat treating to 525 °C in ultra-high purity Argon (UHP-Ar) under inert atmosphere for 8 h. Samples were cut into squares 1.25 × 1.25 × 0.08 cm in size and cleaned by etching in 3 % nitric acid solution. The samples were then rinsed with acetone, polished with 1200 grit (5 μm) SiC polishing paper, and sonicated for 30 min in acetone. Cleaned and polished samples were stored in acetone until application of the polymer coatings. Poly(D,L-lactide-co-glycolide), Mw 30,000–60,000, (Sigma-Aldrich) was dissolved in dichloromethane at 10 and 20 % wt/vol, from here on referred to as AZ31-PLGA 10 %, AZ31-PLGA 20 %, Mg4Y-PLGA 10 % and Mg4Y-PLGA 20 %, respectively, depending on the alloy and polymer concentration utilized. The polished substrates were subsequently dipped into the respective polymer solution at room temperature, allowed to reside for 1 min, withdrawn at a speed of 200 μm/s using a dip coater (Desktop Dip Coater, Model No EQ-HWTL-01-A, MTI Corporation, USA), and then finally allowed to dry at room temperature. This dip coating process was repeated in triplicate on each sample for each test completed.

### 2.2 Characterization of coatings

The coating thickness of the films was calculated by measuring the weight gain from dip coating in polymer

solutions and utilizing the sample dimensions. Thickness measurements were taken in triplicate and averaged. The presence of the coatings was further confirmed by attenuated total reflectance Fourier transform infrared spectroscopy (ATR-FTIR, Nicolet 6700 spectrophotometer, Thermo Electron Corporation) using a diamond ATR Smart orbit. Spectra were obtained at  $1.0\text{ cm}^{-1}$  resolution averaging 32 scans in the  $400\text{--}2,500\text{ cm}^{-1}$  frequency range.

### 2.3 In vitro degradation and corrosion

Electrochemical corrosion characterization studies of the coated alloy samples were performed using CH604A (CH Instruments Inc) electrochemical work station. Following sample preparation as described in the previous section, one side of each sample was connected to a wire with silver epoxy and then electrically insulated, so that only one side is exposed for conducting the electrochemical tests. The length and width measurements were taken for corrosion current calculations. Ag/AgCl and a platinum wire were employed as the reference and counter electrodes, respectively. Testing was carried out utilizing a 3-neck jacketed flask (ACE Glassware) filled with 125 mL Dulbecco's Modified Eagle's Medium (DMEM) containing 10 % fetal bovine serum (FBS, Atlanta Biologicals, Lawrenceville, GA) and 1 % penicillin/streptomycin antibiotics (P/S, Gibco, Grand Island, NY), equilibrated to  $37\text{ }^{\circ}\text{C}$ . All the specimens were allowed to equilibrate to reach a stable open circuit potential (OCP), before initiating the polarization tests at a scan rate of  $1.0\text{ mV/s}$ . The corrosion current was determined using the Tafel extrapolation of the polarization curve and normalized by the exposed surface area to yield a measurement of corrosion current density. The software program Origin with a Tafel packet was used to perform the Tafel extrapolation and plot the data.

Corrosion profile up to 21 days was assessed by analyzing the magnesium ion concentration in media extracted after sample incubation. The coated substrates were sterilized by UV light exposure for 1 h per side. Each substrate was then soaked in 2 mL of DMEM containing 10 % FBS and 1 % P/S under standard growth conditions of  $37\text{ }^{\circ}\text{C}$ , 5 %  $\text{CO}_2$  and 95 % relative humidity for 21 days. The media was changed and collected every 24 h to monitor the degradation rate under in vitro conditions. The collected media was diluted in 0.03 M Tris buffer solution and analyzed using inductively coupled plasma optical emission spectroscopy (ICP-OES, iCAP duo 6500 Thermo Fisher). Magnesium ion concentrations in solution were compared to media and uncoated substrate controls. The coatings were characterized post-corrosion using a digital optical microscope (Keyence VHX-600K) and a scanning electron microscope at 10 kV (SEM, Philips XL30 FEG

ESEM). Samples were sputter coated with palladium (Cressington sputter coater 108A) for observation of the surface morphology post corrosion using SEM.

## 2.4 Cytocompatibility

### 2.4.1 Cell culture

Murine MC3T3-E1 pre-osteoblast cells obtained from ATCC (Manassas, VA) were utilized for cell culture studies. Cells were cultured in minimum essential medium alpha ( $\alpha$ -MEM, Gibco, Grand Island, NY) containing 10 % fetal bovine serum (FBS, Atlanta Biologicals, Lawrenceville, GA) and 1 % penicillin/streptomycin antibiotics (P/S, Gibco, Grand Island, NY) at  $37\text{ }^{\circ}\text{C}$ , 5 %  $\text{CO}_2$  and 95 % relative humidity. Substrates were placed in 12 well plates and sterilized using UV radiation for 40 min on each side. The substrates were then seeded with MC3T3 cells, after third to seventh passage, at a density of 60,000 cells/well, with a total media volume of 2 mL/well. Media was changed every other day throughout the testing period.

### 2.4.2 Live/dead assay

Cell viability was assessed using Live/Dead staining (Invitrogen, Live/Dead Staining Kit). The assays were performed on day 1 and 3 substrate cell cultures. The coated alloy substrates were rinsed with phosphate buffered saline (PBS, Lonza BioWhittaker Buffers and Buffered Salines,  $1\times$ ,  $0.0067\text{ M}(\text{PO}_4)$  without calcium or magnesium) and then incubated for 30 min in live/dead stain, calcein AM and ethidium homodimer-1, diluted in PBS. After incubation, the samples were again washed with PBS and then imaged using fluorescence microscopy (Olympus CKX41, Olympus DP25 Microscope Camera).

### 2.4.3 Cytoskeleton fixing and imaging

Following fluorescence imaging, cells were fixed using a 2.5 % glutaraldehyde solution for 15 min. Fixed samples were then subjected to alcohol dehydration and mounted for SEM imaging. Samples were coated with palladium in order to observe the cell morphology using SEM.

## 3 Results and discussion

### 3.1 Coating characterization

The thickness of the coatings was calculated by measuring the sample dimensions and the gain in weight following dip coating, assuming a fully dense, nonporous coating and the

**Table 1** Coating thicknesses on magnesium substrates

Sample type	Thickness ( $\mu\text{m}$ )
AZ31-PLGA 10 %	$\sim 1.6$
AZ31-PLGA 20 %	$\sim 41.8$
Mg4Y-PLGA 10 %	$\sim 1.6$
Mg4Y-PLGA 20 %	$\sim 62.1$

manufacturer-provided material density of 1.34 g/mL using Eq. 2:

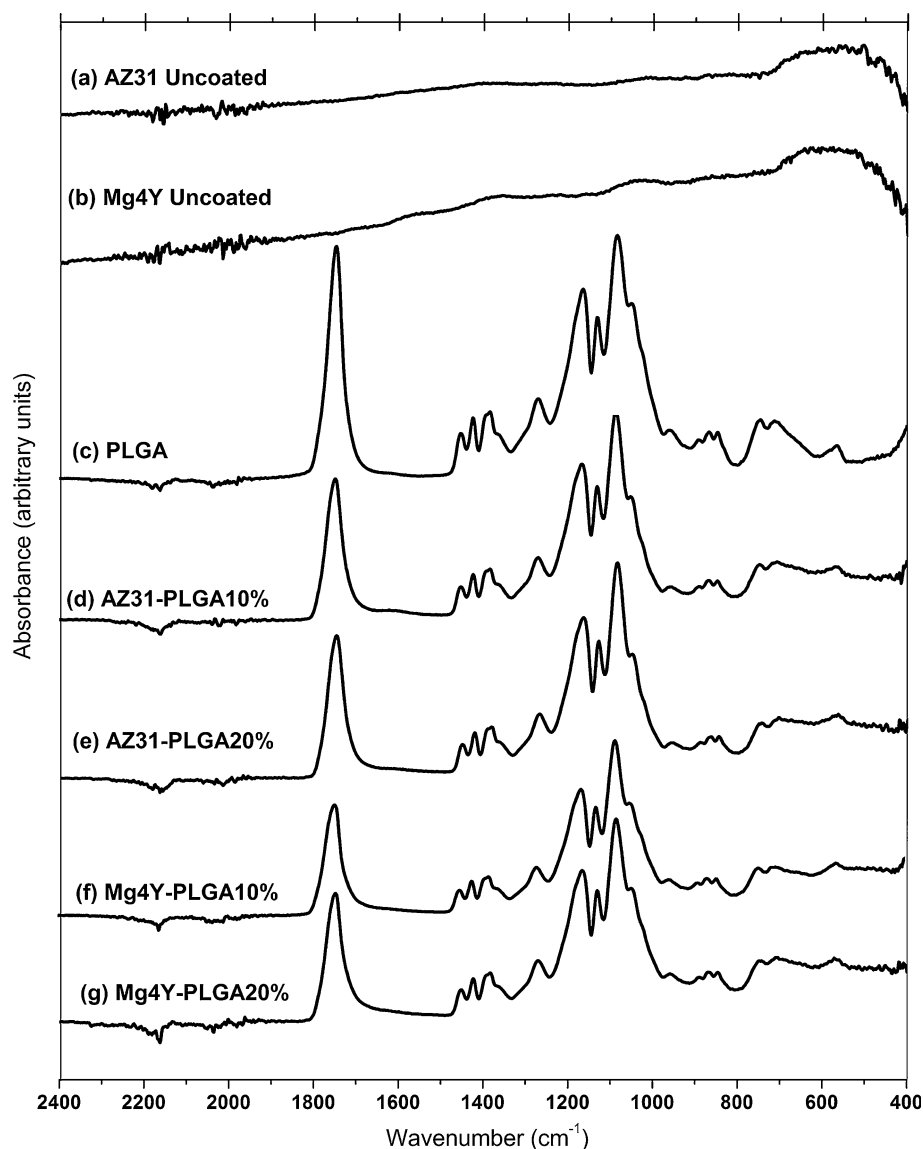
$$\text{Thickness } (\mu\text{m}) = \frac{\text{Weight gain(g)}}{\text{density}\left(\frac{\text{g}}{\text{cm}^3}\right) \times \text{Surface area}(\text{cm}^2)} \times 10^4 \quad (2)$$

Resulting thicknesses indicate that there is a large increase in coating thickness with a higher solution

concentration, (Table 1). There is no statistical difference however between the coating thickness on AZ31 or Mg4Y alloy with either polymer concentrations, indicating similar interaction occurring between the alloy surface and the polymer solution for both alloys.

FT-IR was used to confirm the presence of the polymer coatings on the alloy. Figure 1 shows the FT-IR spectrum of uncoated Mg alloys, PLGA and PLGA coated samples. The characteristic bonds at numerous wave numbers, such as the carbonyl stretching at  $1,750 \text{ cm}^{-1}$ , C–O–C stretching at  $\sim 1,080 \text{ cm}^{-1}$  are indicative of the presence of the PLGA polymer [26]. No such peaks are expectedly seen on the bare metal substrates devoid of the polymer. Differences between the coating thicknesses, as expected, did not appear to influence and cause any changes to the obtained spectra.

**Fig. 1** FTIR spectra of uncoated AZ31 (a), uncoated Mg4Y (b), pure PLGA (c) and coated samples AZ31-PLGA 10 % (d), AZ31-PLGA 20 % (e), Mg4Y-PLGA 10 % (f) and Mg4Y-PLGA 20 % (g), showing clear presence of PLGA on all coated substrates



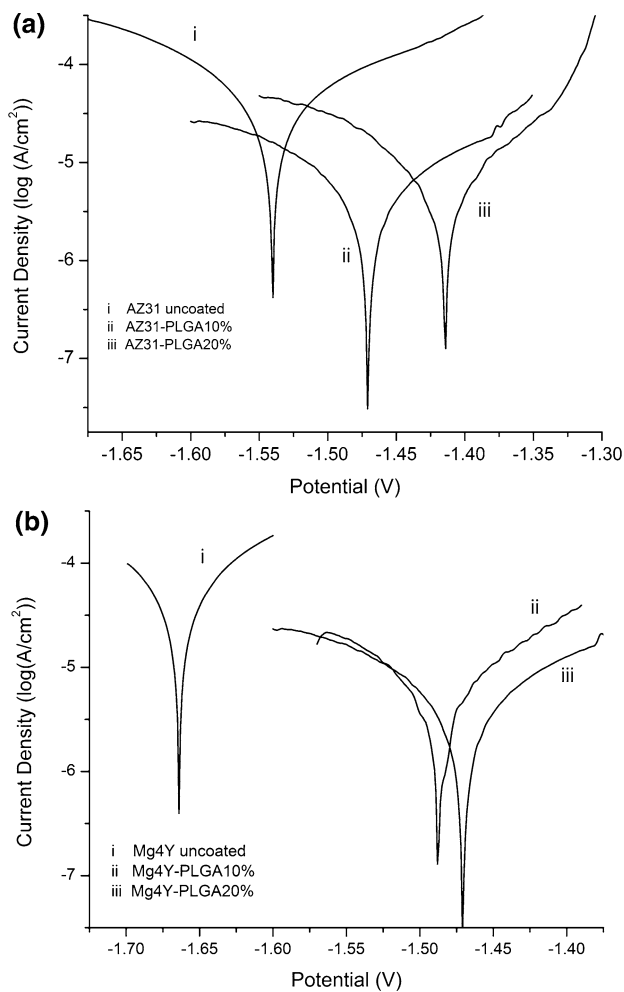


**Fig. 2** Polarization curves of substrates AZ31 **a** uncoated (i), PLGA 10 % (ii) and PLGA 20 % (iii) coatings and Mg4Y **b** uncoated (i), PLGA 10 % (ii) and PLGA 20 % (iii) coatings

**Table 2** Corrosion potential ( $E_{\text{corr}}$ ) and current density ( $i_{\text{corr}}$ ) values for coated and uncoated substrates

	$E_{\text{corr}}$ (V)	$i_{\text{corr}}$ (A/cm <sup>2</sup> )
AZ31-uncoated	-1.54	3.10E-05
AZ31-PLGA 10 %	-1.469	5.20E-06
AZ31-PLGA 20 %	-1.415	6.05E-06
Mg4Y-uncoated	-1.664	4.42E-05
Mg4Y-PLGA 10 %	-1.485	8.09E-06
Mg4Y-PLGA 20 %	-1.469	6.85E-06

3.2 In vitro degradation

Polarization curves for the coated and uncoated substrates can be seen in Fig. 2 for AZ31 substrates (a) and Mg4Y substrates (b). Table 2 gives a summary of the corrosion potential and corrosion current densities as calculated from extrapolation of the Tafel plots. For the AZ31 alloy, PLGA

coatings on the substrates resulted in an  $E_{\text{corr}}$  that is less negative than the uncoated alloy, indicating that the coating did provide a barrier for corrosion. Increase in polymer thickness further yielded an increase in  $E_{\text{corr}}$  indicating the beneficial influence of the thicker polymer coating. The presence of the polymer coatings on AZ31 visibly lowered the  $i_{\text{corr}}$  values compared to the uncoated AZ31 alloy substrate, although there was no significant variation between the two different polymer concentrations and thickness of the polymer coatings. The addition of PLGA coatings on Mg4Y alloy substrates also resulted in  $E_{\text{corr}}$  values which are less negative than the uncoated substrates as well as reductions in  $i_{\text{corr}}$  values similar to the coatings on AZ31. Similar to the coatings on the AZ31 substrate, there was no perceivable difference in the  $i_{\text{corr}}$  values between the two polymer concentrations and consequent thickness of the polymer coatings. Additionally, unlike the coatings on AZ31, increasing the thickness of the PLGA coating on Mg4Y substrates did not offer much change in the  $E_{\text{corr}}$  or  $i_{\text{corr}}$  values. It should be however noted that the corrosion potential of the uncoated Mg4Y is more negative compared to the uncoated commercial AZ31 alloy indicative of a more reactive alloy surface, which is not consistent with predictions reported by previous researchers [20]. This is possibly a consequence of the difference in the processing conditions of the alloys. AZ31 is a commercial product that has been likely processed with better precision, subjected to commercial extrusion and rolling procedures, and likely better impurity control than the laboratory-generated Mg4Y that was not subjected to any further processing modifications following casting other than the standard homogenization treatments. Despite these differences between the two alloy substrates to begin with, overall however, the polarization curves of the polymer coated AZ31 and Mg4Y substrates do exhibit corrosion protection of the bare AZ31 and Mg4Y alloys as demonstrated by a less negative  $E_{\text{corr}}$  values as well as a reduction in  $i_{\text{corr}}$  values for all the coated substrates regardless of the thickness and the polymer concentration.

Coated and uncoated substrates were further immersed in DMEM with FBS and P/S which was changed daily and maintained under in vitro conditions to qualitatively determine the effect of polymeric coatings on the stability and the degradation rate of the alloys. SEM images of the coated substrates of AZ31 and Mg4Y are shown in Figs. 3 and 4 respectively, at three time points namely, 3, 12 and 15 days. At day 3, microscopic inspection indicates that the coatings on all substrates are present; however noticeable changes to the substrate surface begin to appear particularly with the coatings corresponding to higher polymer concentration and higher thickness. Coatings of PLGA 10 % show the onset of corrosion under the surface, as indicated by the plate-like morphology typical of the

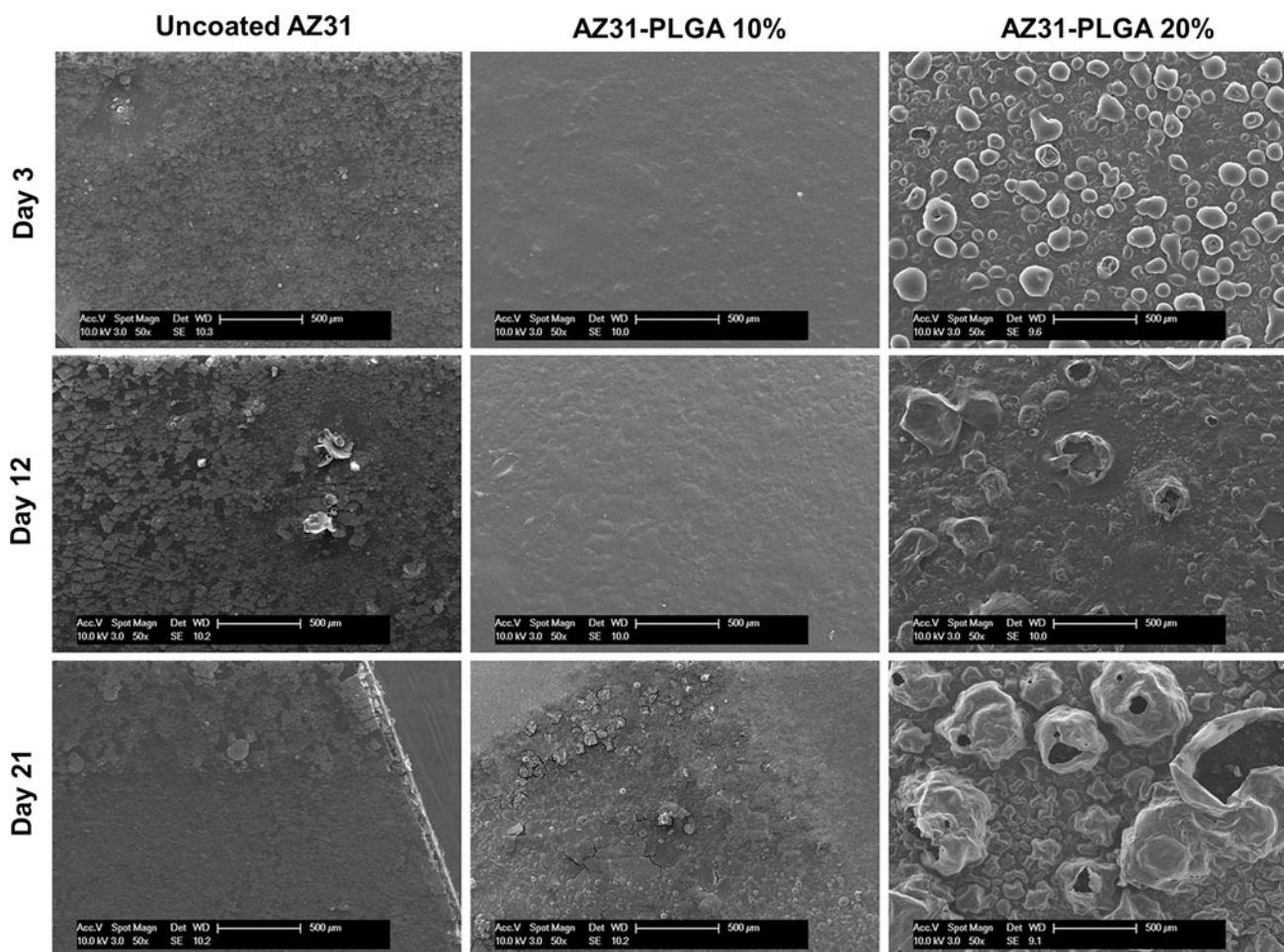


**Fig. 3** SEM images of uncoated and PLGA coated AZ31 substrates post incubation in media (Scale bar is 500  $\mu\text{m}$ )

magnesium corrosion product which is also seen in the AZ31 and Mg4Y uncoated substrates. Comparing the PLGA 10 % coated substrates with the uncoated substrates, the coatings appear to slow the corrosion for shorter time points. The corrosion however progresses with increase in incubation time. Coatings of PLGA 20 % show the formation of gas bubbles, likely of trapped hydrogen gas, forming underneath the polymeric surface during 3 days of incubation. As the incubation time progresses, these bubbles appear to grow with increasing volume of gas generated reaching the maximum pressure leading to collapse of the gas bubbles, consequently leaving the unprotected substrate fully exposed in some areas to the liquid environment while the polymer remains intact in other non-specific areas. The same plate-like corrosion product can be seen on the exposed areas of the substrate. This effect appears to be especially aggravated on the Mg4Y-PLGA 20 % surface. The Mg4Y alloy appears to undergo more aggressive corrosion in the presence of PLGA in contrast to the AZ31 alloy. Previous research indicates that an opposite effect should be true in the uncoated alloys [20].

However, to the authors knowledge, these two alloys, with or without coatings, have not been directly compared. For all polymer coatings, the polymer provides partial protection of the alloy surface initially, but the stability of the coating appears to break down with subsequent incubation time leading to eventual swelling, deformation, and eventual delamination of the polymer from the alloy surface.

ICP was used to determine ionic concentrations of magnesium in the DMEM collected in order to further evaluate the degradation of the AZ31 and Mg4Y substrates when coated with the protective PLGA polymer (Fig. 5a, b). For all samples, including uncoated substrates, there is an increase in magnesium ion concentration above pure media baseline. Both AZ31-PLGA 10 % and Mg4Y-PLGA 10 % coatings show some reduction in magnesium ion release at day 3, and at subsequent time points AZ31-PLGA 10 % coatings yield magnesium concentrations similar to the uncoated substrate for subsequent time points until day 12 beyond which the magnesium ion concentration appear to be slightly elevated compared to the uncoated AZ31 alloy. For AZ31-PLGA 20 % and Mg4Y-PLGA 20 %,

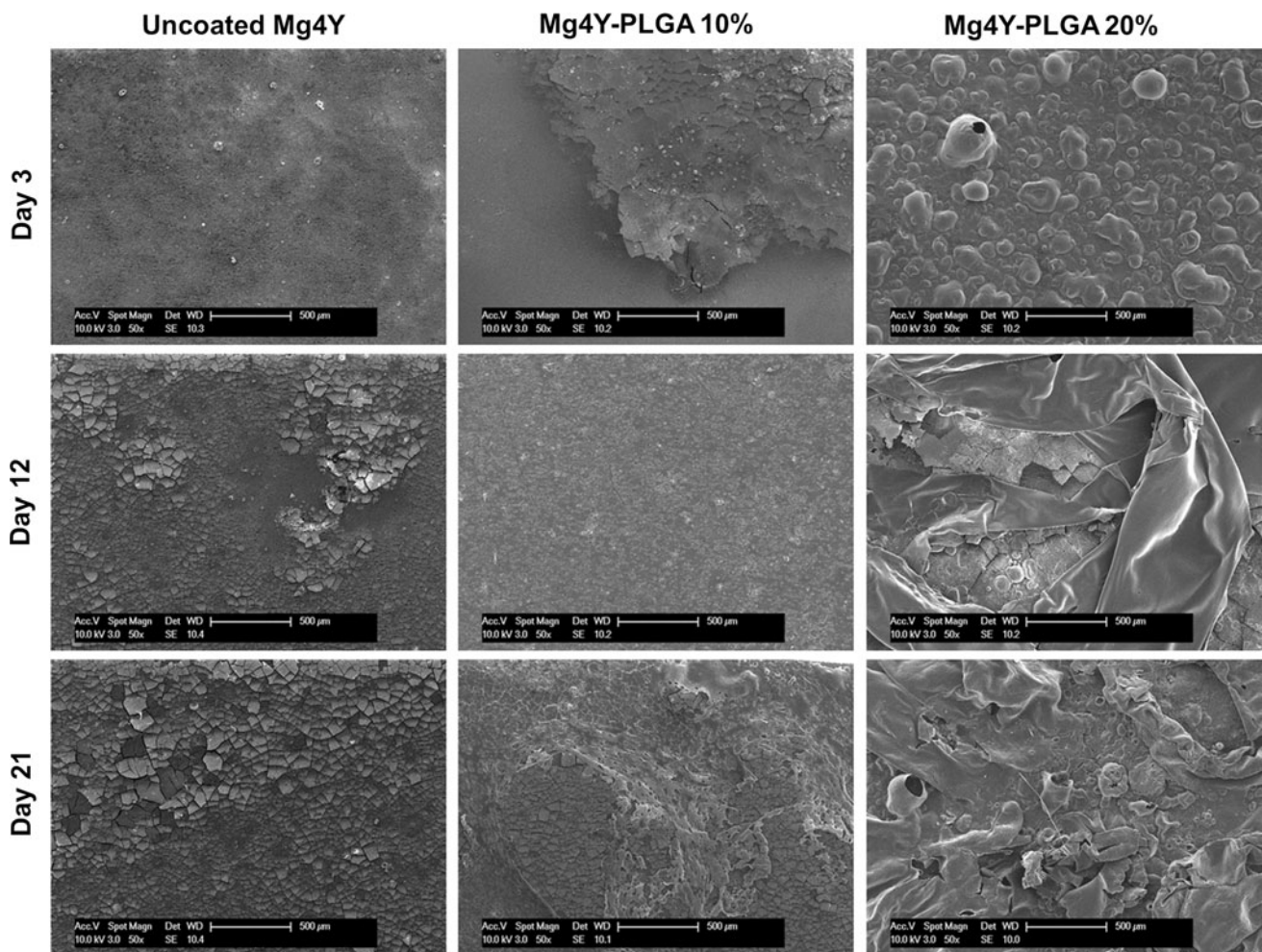


**Fig. 4** SEM images of uncoated and PLGA coated Mg4Y substrates post incubation in media (Scale bar is 500  $\mu\text{m}$ )

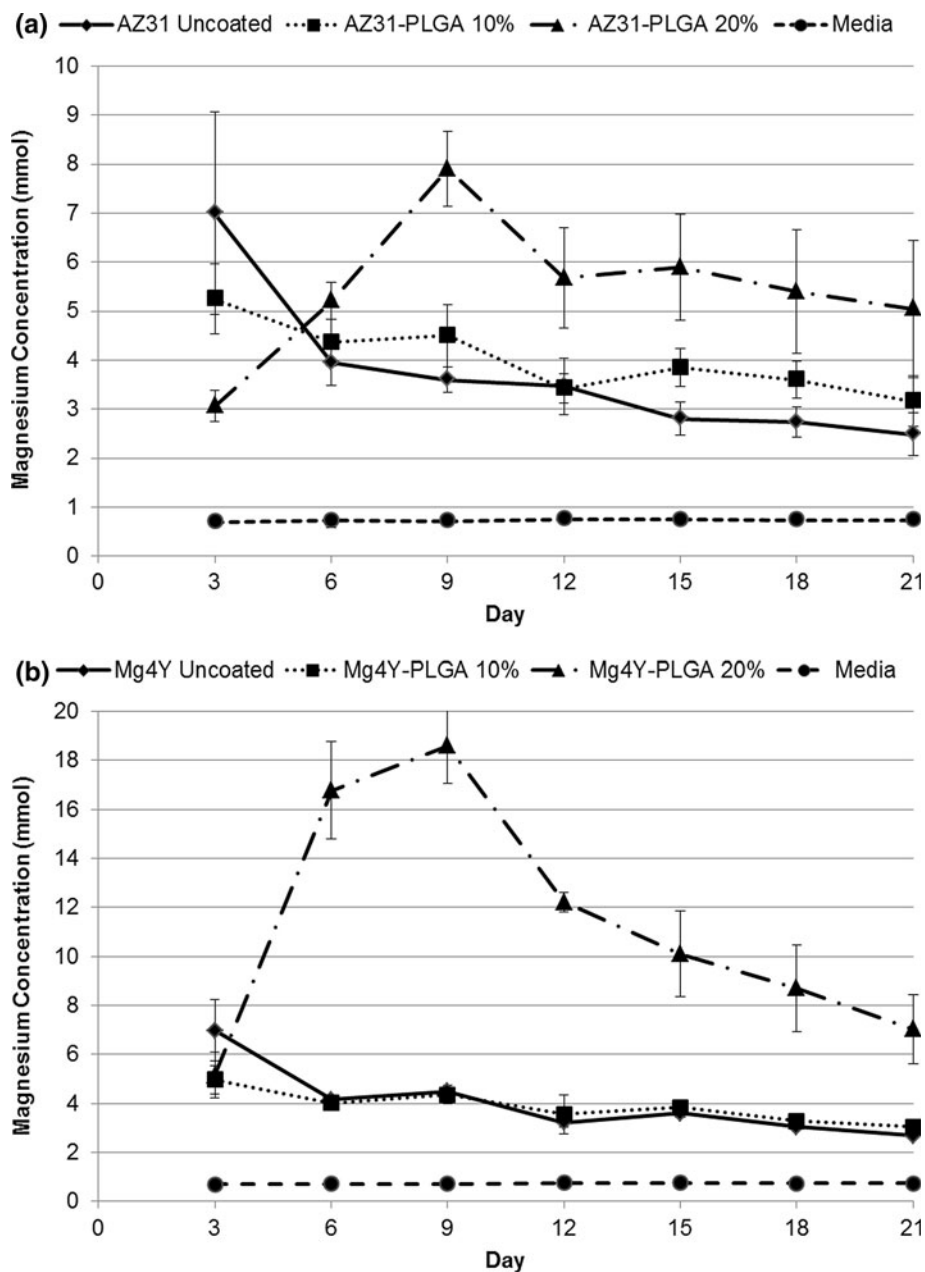
there is again a reduction in magnesium ion release in comparison to the uncoated substrates at day 3. However, at later time points this reduction is not maintained. The PLGA 20 % coatings on both substrates appear antagonistic, with the daily ion release rate increasing rapidly until day 9 above that of the uncoated substrates with the Mg4Y-PLGA 20 % exhibiting almost two-fold higher dissolution of Mg compared to the corresponding coating on AZ31. This is unexpected because as corrosion of the metal alloy underneath the PLGA coating proceeds, pH should increase, pushing the surface closer to passivation [2]. This would in turn reduce the corrosion because the buildup of the more robust magnesium hydroxide layer would lead to some corrosion protection for the alloy surface [27].

It is also important to note that PLGA is considered semi-permeable to water, as the water penetration into the bulk of the polymer occurs faster than surface hydrolytic degradation of the polymer [28]. It is well known that the hydrolytic degradation within the bulk of the PLGA coating would result in the formation of acidic byproducts.

These byproducts could react with the magnesium corrosion ions or magnesium hydroxide, forming soluble magnesium lactates or magnesium glycolates. The formation of lactates and glycolates will prevent the formation and growth of dense and thick corrosion protective magnesium hydroxide layer. It is therefore very unlikely that the reaction products of magnesium lactate and glycolate can form dense corrosion protective layers as these salts are more soluble than magnesium hydroxide [29, 30]. The local increase in pH as well as absence of any corrosion protective layer will therefore lead to the rapid corrosion of the underlying bare surfaces. The effect is expected to be greater with the thicker coating, thus explaining the greater corrosion seen with the PLGA 20 % coatings.

The corrosion results observed by us compare well with the observation of the coating tests reported by Chen et al. [14], wherein PCL and PLA coatings on pure magnesium displayed a “special interaction”. The authors observed that the individual degradations of the polymer coating and the magnesium alloy were each antagonistic of the other and that this reciprocity ultimately undermined the corrosion

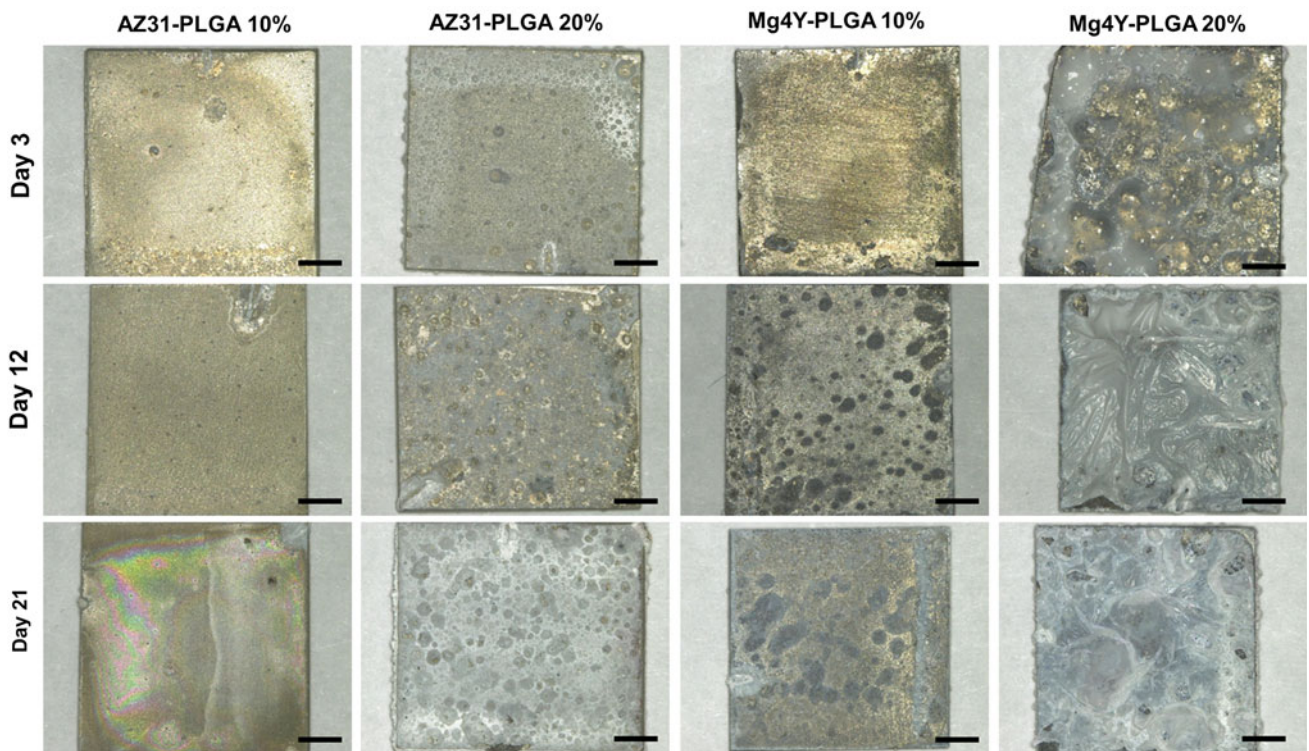
**Fig. 5** ICP measurements of daily magnesium ion concentration in extracted incubation media for AZ31 coated and uncoated samples (a) and Mg4Y coated and uncoated samples (b)



resistance of the material under dynamic degradation tests. The hypothesized effect reported by Chen et al. correlates well with the ICP results of day 3 reported here as well as the electrochemical corrosion results, which assess that the corrosion protection by the PLGA coating on AZ31 and Mg4Y is only observed at very early time points, demonstrating that the PLGA coatings regardless of the concentration only serve to provide a physical barrier to corrosion, through day 3, but that the protection is not maintained beyond 6 days of incubation, presumably due to the penetration of water into the PLGA bulk coating and the subsequent degradation of both the polymer coating and the magnesium alloy substrate with the formation of the soluble products outlined above. The discussed mechanism is also consistent with the SEM

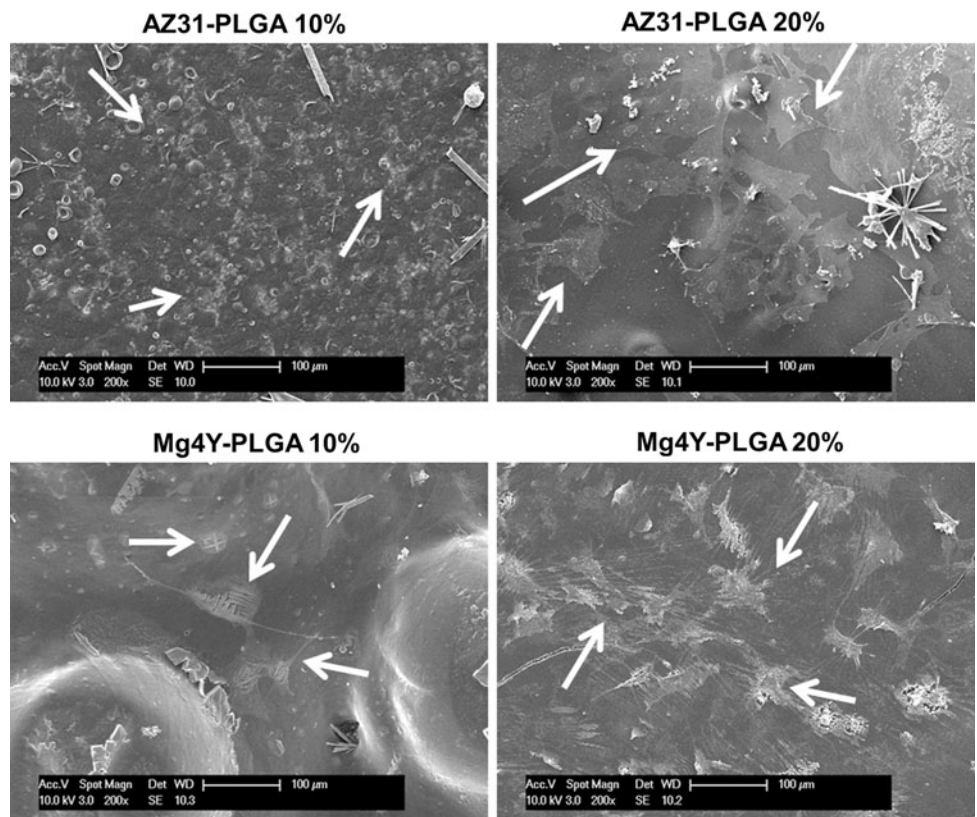
observations, which clearly show the formation of large number of hydrogen gas bubbles in AZ31 PLGA 20% and Mg4Y PLGA 20% coatings in contrast with the corresponding AZ31 and Mg4Y substrates containing PLGA 10% coatings (see Figs. 3, 4).

Figure 6 shows the digital optical images of the incubated substrates at the same three time points as shown in the SEM images. These images also support the previous observations of coating protection and durability, including the formation of bubbles beneath the polymer (day 3 PLGA 20% on AZ31 and Mg4Y), the separation of the thicker coatings from the alloy surface (especially PLGA 20% on Mg4Y) and the more aggressive corrosion of Mg4Y in comparison to AZ31.



**Fig. 6** Digital optical images of PLGA coated AZ31 and Mg4Y substrates post incubation in media (*Scale bar is 2 mm*)

**Fig. 7** Morphology of MC3T3 osteoblasts at 24 h post-seeding, indicating better cell adhesion for thicker PLGA coatings (*Scale bar is 100 μm*)



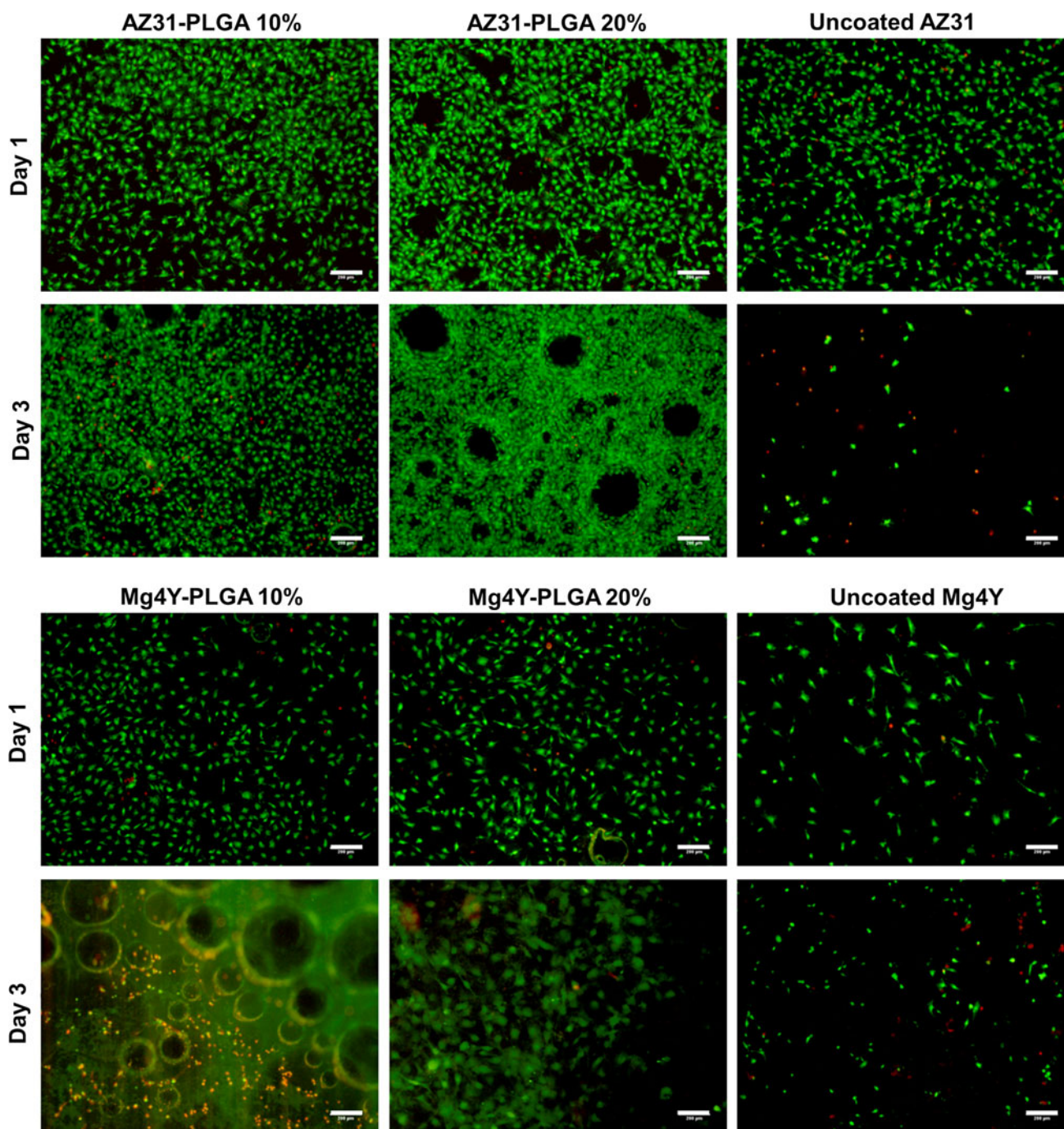


**Fig. 8** Live/Dead staining of MC3T3 osteoblasts on coated and uncoated substrates indicating improved biocompatibility of coated substrates over uncoated substrates (Scale bar is 200  $\mu\text{m}$ )

### 3.3 Cytocompatibility

SEM images of cells fixed on the surface of the alloys 24 h following seeding can be seen in Fig. 7 and the Live/Dead staining of osteoblasts at 1 and 3 days post seeding can be seen in Fig. 8. These SEM images show the cell cytoskeletons, indicated by the arrows, flattened and extended on the polymeric surface, indicating good adhesion of the

osteoblasts validating the polymer coated surface being favorable for cell attachment. Staining of cells at 1 and 3 days (Fig. 8) shows an increase in cell number at day 3 over day 1, indicating no inhibition for cell proliferation, especially for the polymer coated AZ31 substrates. It appears therefore that the formation of gas bubbles in the polymer plays a direct role in the location and the manner in which the cells grow. For example, AZ31-PLGA 20 %

at day 3 shows open regions where the hydrogen bubbles resulting from corrosion have burst open preventing attachment of the cells. Surrounding the gas pocket are areas of high density of cells, but within the spherical gas bubble pocket regions no cells have proliferated. Additionally, as seen in Mg4Y-PLGA 10 % at day 3, where cells may have proliferated within the spherical gas pocket region following collapse of the gas bubbles or underneath the polymeric coating, those cells do not survive. This is likely due to the change in local ion concentrations due to soluble by-products formed as discussed above. It should be noted however that the application of PLGA coatings on the surface of AZ31 and Mg4Y alloys despite the time dependent corrosion protection demonstrated in Figs. 3 and 4, has a clear improvement on the biocompatibility of the uncoated alloy surface showing improved cell viability and proliferation over the uncoated substrates.

Compiling the various corrosion and cell adhesion, viability and proliferation results outlined above, it is clear that although the biocompatibility of the PLGA coating is better, the corrosion protective nature of PLGA coatings on the surface of magnesium alloys however is inconsistent. While numerous factors affect the degradation rate of PLGA polymers, the crucial issue with utilizing PLGA (and many other degradable synthetic polymers) as a temporary tool for corrosion protection is the mechanism of PLGA degradation. PLGA is known to undergo bulk erosion *in vivo*, wherein the full body of the material is simultaneously attacked by water, as opposed to surface erosion, where only the surface of the material is degraded [28]. In the context of protecting metallic surfaces from corrosion, the bulk erosion of the polymeric coating leads to rapid exposure of the surface to water and consequent formation of acidic erosion byproducts. Thus, the amount of water exposure to the underlying bare metal surfaces is limited but not fully prevented. This appears to be exaggerated by the evolution of hydrogen gas upon initiation of corrosion. The gas is trapped below the polymeric coating, forming gas pockets which burst and expose larger areas of the metallic substrate to aqueous attack. Further studies and optimized coating strategies to increase the alloy surface-polymer coating adhesion may yield improved corrosion resistance because an increased adhesion would reduce or eliminate gas pocket formation between the polymer and alloy. These studies are currently in progress and the results will be reported subsequently.

#### 4 Conclusion

A 50:50 PLGA polymer with two different concentrations was coated onto the surface of both AZ31 and Mg4Y alloys through a solution dip-coating method. The implementation

of PLGA yielded homogeneous and reliable coatings on AZ31 and Mg4Y alloy substrates offering some level of immediate corrosion protection over a limited time period. However, once the aqueous corrosion attack is initiated, the polymer offers little protection over subsequent time periods although dramatic improvements in osteoblast adhesion and proliferation are observed on the surface of both alloy substrates. Between the two alloys, Mg4Y substrates, both coated and uncoated, appear less resistant to corrosion in comparison to AZ31 substrates, which is in direct contrast with results from previous studies. Preventing the formation of gas pockets below the polymeric coatings, through increased alloy-polymer adhesion, may lead to improved corrosion resistance rendering the implementation of these coated Mg alloy substrates for possible use in orthopedic fixation plate application while also permitting the utilization of PLGA for additional biotechnological applications such as drug delivery.

**Acknowledgments** The authors gratefully acknowledge the support of National Science Foundation, NSF (Grant # CBET-0933153) and the Engineering Research Center funded by the National Science Foundation, NSF-ERC (Grant # EEC-0812348). The authors also acknowledge the financial support of the Center for Complex Engineered Multifunctional Materials (CCEMM), University of Pittsburgh for support of equipment, supplies and reagents used in this research. PNK also acknowledges the support of the Edward R. Weidlein Chair Professorship funds for partial support of miscellaneous research related expenditures. Additionally, the authors would like to thank the Department of Mechanical Engineering and Materials Science for the provision of access to the electron microscopy instrumentation and for assistance with the execution of this part of our research.

#### References

1. Staiger MP, Pietak AM, Huadmai J, Dias G. Magnesium and its alloys as orthopedic biomaterials: a review. *Biomaterials*. 2006;27(9):1728–34. doi:10.1016/j.biomaterials.2005.10.003.
2. Zeng R, Dietzel W, Witte F, Hort N, Blawert C. Progress and challenge for magnesium alloys as biomaterials. *Adv Eng Mater*. 2008;10(8):B3–14. doi:10.1002/adem.200800035.
3. Witte F. The history of biodegradable magnesium implants: a review. *Acta Biomater*. 2010;6(5):1680–92. doi:10.1016/j.actbio.2010.02.028.
4. Witte F, Hort N, Vogt C, Cohen S, Kainer KU, Willumeit R, et al. Degradable biomaterials based on magnesium corrosion. *Curr Opin Solid State Mater Sci*. 2008;12(5–6):63–72. doi:10.1016/j.cossms.2009.04.001.
5. Xin Y, Hu T, Chu PK. *In vitro* studies of biomedical magnesium alloys in a simulated physiological environment: a review. *Acta Biomater*. 2011;7(4):1452–9. doi:10.1016/j.actbio.2010.12.004.
6. Wang Y, Wei M, Gao JC. Improve corrosion resistance of magnesium in simulated body fluid by dicalcium phosphate dihydrate coating. *Mater Sci Eng C Biomimetic Supramol Syst*. 2009;29(4):1311–6. doi:10.1016/j.msec.2008.09.051.
7. Witte F, Fischer J, Nellesen J, Crostack HA, Kaese V, Pisch A, et al. *In vitro* and *in vivo* corrosion measurements of magnesium alloys. *Biomaterials*. 2006;27(7):1013–8. doi:10.1016/j.biomaterials.2005.07.037.

8. Zberg B, Uggowitzer PJ, Loeffler JF. MgZnCa glasses without clinically observable hydrogen evolution for biodegradable implants. *Nat Mater*. 2009;8(11):887–91. doi:10.1038/nmat2542.
9. Kirkland NT, Birbilis N, Staiger MP. Assessing the corrosion of biodegradable magnesium implants: a critical review of current methodologies and their limitations. *Acta Biomater*. 2012;8(3):925–36. doi:10.1016/j.actbio.2011.11.014.
10. de Jonge LT, Leeuwenburgh SCG, Wolke JGC, Jansen JA. Organic-inorganic surface modifications for titanium implant surfaces. *Pharm Res*. 2008;25(10):2357–69. doi:10.1007/s1095-008-9617-0.
11. Roy A, Singh SS, Datta MK, Lee B, Ohodnicki J, Kumta PN. Novel sol-gel derived calcium phosphate coatings on Mg4Y alloy. *Mater Sci Eng B Adv Funct Solid State Mater*. 2011;176(20):1679–89. doi:10.1016/j.mseb.2011.08.007.
12. Kannan MB. Enhancing the performance of calcium phosphate coating on a magnesium alloy for bioimplant applications. *Mater Lett*. 2012;76:109–12. doi:10.1016/j.matlet.2012.02.050.
13. Wong HM, Yeung KWK, Lam KO, Tam V, Chu PK, Luk KDK, et al. A biodegradable polymer-based coating to control the performance of magnesium alloy orthopaedic implants. *Biomaterials*. 2010;31(8):2084–96. doi:10.1016/j.biomaterials.2009.11.111.
14. Chen Y, Song Y, Zhang S, Li J, Zhao C, Zhang X. Interaction between a high purity magnesium surface and PCL and PLA coatings during dynamic degradation. *Biomed Mater*. 2011;6(2):025005. doi:10.1088/1748-6041/6/2/025005.
15. Guo M, Cao L, Lu P, Liu Y, Xu X. Anticorrosion and cytocompatibility behavior of MAO/PLLA modified magnesium alloy WE42. *J Mater Sci Mater Med*. 2011;22(7):1735–40. doi:10.1007/s10856-011-4354-z.
16. Langer R. Drug delivery and targeting. *Nature*. 1998;392(6679):5–10.
17. Jain RA. The manufacturing techniques of various drug loaded biodegradable poly(lactide-co-glycolide) (PLGA) devices. *Biomaterials*. 2000;21(23):2475–90. doi:10.1016/s0142-9612(00)00115-0.
18. Park TG. Degradation of poly(lactic-co-glycolic acid) microspheres: effect of copolymer composition. *Biomaterials*. 1995;16(15):1123–30. doi:10.1016/0142-9612(95)93575-x.
19. Valimaa T, Laaksovirta S. Degradation behaviour of self-reinforced 80L/20G PLGA devices in vitro. *Biomaterials*. 2004;25(7–8):1225–32. doi:10.1016/j.biomaterials.2003.08.072.
20. Drynda A, Deinet N, Braun N, Peuster M. Rare earth metals used in biodegradable magnesium-based stents do not interfere with proliferation of smooth muscle cells but do induce the upregulation of inflammatory genes. *J Biomed Mater Res A*. 2009;91A(2):360–9. doi:10.1002/jbm.a.32235.
21. Kim K, Luu YK, Chang C, Fang DF, Hsiao BS, Chu B, et al. Incorporation and controlled release of a hydrophilic antibiotic using poly(lactide-co-glycolide)-based electrospun nanofibrous scaffolds. *J Controlled Release*. 2004;98(1):47–56. doi:10.1016/j.jconrel.2004.04.009.
22. Jeon O, Song SJ, Kang SW, Putnam AJ, Kim BS. Enhancement of ectopic bone formation by bone morphogenetic protein-2 released from a heparin-conjugated poly(L-lactic-co-glycolic acid) scaffold. *Biomaterials*. 2007;28(17):2763–71. doi:10.1016/j.biomaterials.2007.02.023.
23. Li JN, Cao P, Zhang XN, Zhang SX, He YH. In vitro degradation and cell attachment of a PLGA coated biodegradable Mg–6Zn based alloy. *J Mater Sci*. 2010;45(22):6038–45. doi:10.1007/s10853-010-4688-9.
24. Xu X, Lu P, Guo M, Fang M. Cross-linked gelatin/nanoparticles composite coating on micro-arc oxidation film for corrosion and drug release. *Appl Surf Sci*. 2010;256(8):2367–71. doi:10.1016/j.apsusc.2009.10.069.
25. Lu P, Fan H, Liu Y, Cao L, Wu X, Xu X. Controllable biodegradability, drug release behavior and hemocompatibility of PTX-eluting magnesium stents. *Colloids Surf B*. 2011;83(1):23–8. doi:10.1016/j.colsurfb.2010.10.038.
26. Paragkumar NT, Edith D, Six J-L. Surface characteristics of PLA and PLGA films. *Appl Surf Sci*. 2006;253(5):2758–64. doi:10.1016/j.apsusc.2006.05.047.
27. Hornberger H, Virtanen S, Boccaccini AR. Biomedical coatings on magnesium alloys: a review. *Acta Biomater*. 2012;. doi:10.1016/j.actbio.2012.04.012.
28. von Burkersroda F, Schedl L, Gopferich A. Why degradable polymers undergo surface erosion or bulk erosion. *Biomaterials*. 2002;23(21):4221–31.
29. Liu S-T, Nancollas GH. The crystallization of magnesium hydroxide. *Desalination*. 1973;12:75–84.
30. Manzurola E, Apelblat A. Solubilities of L-glutamic acid, 3-nitrobenzoic acid, p-toluic acid, calcium-L-lactate, calcium gluconate, magnesium-DL-aspartate, and magnesium-L-lactate in water. *J Chem Thermodyn*. 2002;34(7):1127–36. doi:10.1006/jcht.2002.0975.